DAMAGE SIMULATIONS IN A COMPOSITE Ω-STIFFENED PANEL IN POSTBUCKLING REGIME

Antonio Blázquez[1], José Reinoso[1], Federico París[1]

[1]Departamento de Mecánica de Medios Continuos y Teoría de Estructuras, Escuela Técnica Superior de Ingeniería, Universidad de Sevilla, Camino de los Descubrimientos s/n, Sevilla, Spain
Email: abg@us.es, jreinoso@us.es, fparis@us.es Web Page: http://www.germus.es

Keywords: postbuckling, stiffened panel, global-local analysis, interlaminar damage

Abstract
Submodeling global-local technique is used in this work to simulate the initiation and development of skin-stringer debonding of a multi-stringer composite stiffened panel subjected to uniaxial compressive loading. In a first step, a geometrical non-linear global like-shell model is used to obtain the deformed pattern evolution. This data is used as kinematic boundary conditions in subsequent local models, one for each stringer, at the central bay of the panel; in these local models, damage around the surface between stringer and skin is modeled by cohesive elements. Experimental data are used for comparison purpose, showing the applicability of the proposed strategy for complex structures.

1. Introduction

As a consequence of the high slenderness of the skin, composite stiffened panels under compressive and shear loadings are prone to undergo significant structural instabilities prior to the failure. The dents appearing along the postbuckling regime lead to the potential initiation and development of skin-stringer debonding at different locations, which principally promotes the specimen collapse.

The simulation of the process presents many difficulties when trying to predict the behavior of a particular panel because of the high sensitibity of the evolution with respect to the initial imperfections of the panel, mainly the geometrical ones [1–3]. Additionally, panels failure is usually catastrofic and characterized by general debonding of the stringers in aside from delaminations and intralaminar damage [4, 5].

In this work, submodeling global-local technique [6] is used for the analysis of a multi-stringer composite stiffened panel subjected to uniaxial compressive loading till collapse. In a first step, a deformed pattern evolution is obtained using a global model considering geometrical nonlinearities. In this step, the perturbation of the ideal geometry is introduced by a combination of several buckling modes. This evolution is used as kinematic boundary conditions in subsequent local models for each stringer. In these local models, damage at the interface between stringer and skin is considered by means of standard cohesive model obeying a linear degradation evolution. Computational damage predictions are compared with experimental data, showing the applicability of the proposed strategy for complex structures.

2. Panel description

The analyzed specimen was a cylindrical panel, length 2708 mm, width 1100 mm and curvature radius 1900 mm. It had 3 Ω-stringers and 4 frames with C-section, see Fig. 1. Stringers were continuous along

Excerpt from ISBN 978-3-00-053387-7

the full length of the panel, distance between their central lines being 220 mm. The frames, which were separated 635 mm each other, had three cut-outs to allow the stringers to run through them.

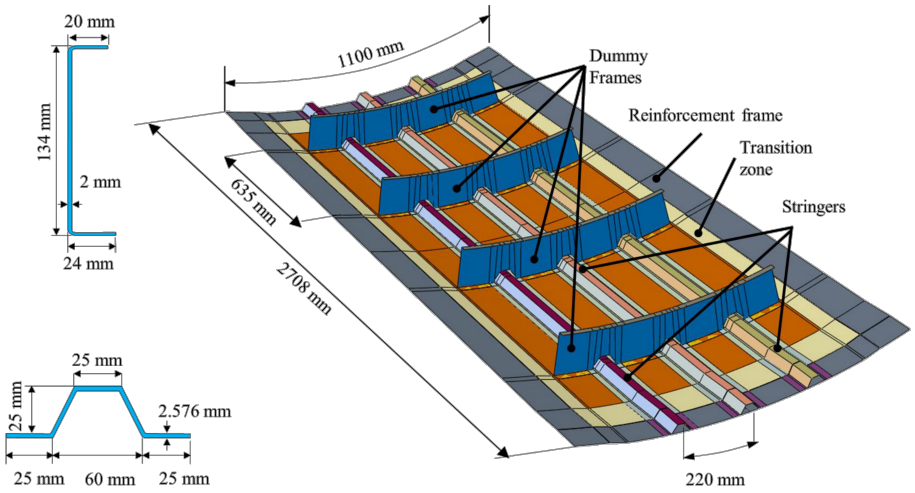

Figure 1. Geometry of the panel.

Both skin and stringers were manufactured using unidirectional carbon fiber epoxy pre-preg material IMA/M21E. Thickness of one ply is 0.184 mm, and stiffness properties are shown in Table 1 (1-direction being fibre direction and 3-direction being normal to the ply). Table 2 shows the stacking sequence for each part of the panel, zero-degree oriented along the axial direction of the panel.

Table 1. Properties of stiffness of a IMA/M21E material ply.

E_1	E_2	E_3	G_{12}	G_{13}	G_{23}	ν_{12}
154 GPa	8.5 GPa	8.5 GPa	4.2 GPa	4.65 GPa	3.0 GPa	0.32

Table 2. Stacking sequence of the panel.

Region	Laminate
Skin	$[45/-45/0/90/-45/45]_S$
Skin frame	$[45/-45/0/-45/45/90/45/-45/0/45/45/90/45/-45/0/-45/45/90/45/-45/0/90/0]_\$$
Stringers	$[45/-45/0/0/0/90/0]$

Stringers were co-bonded to the skin including an adhesive layer of 0.3 mm thickness of Loctite-Henkel Hysol 9695 (Z15435). Table 3 shows the stiffness, strength and toughness properties of this adhesive, which was considered cuasi-isotropic.

3. Experimental test

Details about the experimental test are reported in [7]. Compressive axial load was applied by a vertical hydraulic jack of 35 MN at the extremes of the panel, which were embedded in respective boxes made

Excerpt from ISBN 978-3-00-053387-7

Table 3. Properties of stiffness, strength and toughness of Loctite-Henkel Hysol 9695 (Z15435).

E	ν	σ_{Ic}	$\tau_{IIc} = \tau_{IIIc}$	G_{Ic}	$G_{IIc} = G_{IIIc}$
4.94 GPa	0.3	29.7 MPa	50 MPa	325 J/m^2	850 J/m^2

of aluminum and intended reproducing fully clamped conditions. A pair of guides avoid the longitudinal edges to move perpendicular to the panel. A displacement transducer, 20 strain gages disposed axially and 4 rosettes were used to monitorize the test (the position of some of them can be seen in Fig. 2).

Fig. 2 shows a view of the central part of the specimen. Debondigs between the stringer flanges and the skin were measured and corresponding values (in mm) appear in the picture (560, 400, 200, 140, 103 and 80). The debonded area at the left stringer was large while at that on the right was relatively small and the central one had an intermediate situation. Intralaminar failure is also clearly identified.

Figure 2. View of the central part of the specimen after colapse.

4. Numerical model: global-local strategies

Finite Element is the most popular numerical method to predict the behaviour of complex structural problems, as is the case of postbuckling evolutions of panels loaded in compressive, shear or mixed loads. At present, many works focus their attention on the accurately reproduction of the general response of the panel [3, 5], which is very sensitive to the actual geometry of the panel. More recently, computational techniques such as virtual crack closure technique, cohesive zone models, continuum damage mechanics, see [7–9], have been incorporated to model interlaminar and intralamaninar failure. However, for multi-stringer panels the required computational costs made the use of these features rather impractical. Global-local methodologies provide a competitive strategy that could extend the range of applicability of the techniques for the simulation of damage, thus allowing the estimation of the actual colapse load.

Global-local strategies connect several finite element models of different size that reproduce, with different range of fidelity, the behaviour of the structure. Connection between the different models can be carried out in different ways; in this work submodeling technique of the commercial software Abaqus® was selected. This is a one-way coupling technique: firstly, the global model is solved, after that, its solution is appllied as kinematic conditions along the boundaries of the local model, which is solved in a

Excerpt from ISBN 978-3-00-053387-7

second step. Thus, the global model affects the local one, but not inversely [6].

The numerical model developed in this work is able to reproduce the postbuckling evolution of a particular panel including stringers debonding. Thus, the model considers: geometrical non-linearities, actual geometry and interlaminar damage. These characteristics were considered at different levels: (1) geometrical non-linear formulation was considered at both global and local levels, (2) the geometry of the model was adjusted to that of the actual panel in the global model (by a combination of buckling modes), but not in the local one, and (3) finally, interlaminar damage was only incorporated in the local model.

5. Gobal model: consideration of geometric imperfections

5.1. Global finite element model

Due to the geometry of the panel, a shell-like model was considered for the global level. Though not strictly necessary in this case, adhesive was modeled as a thin layer of solid element. It is the experience of the authors [3] that, in this way, a qualitatively estimation of the distribution of transversal stress components (σ_{33}, τ_{13} and τ_{23}, 3-direction being normal to the layer) can be obtained; these data can be considered in order to define the size and location of the local model. Thus, the global model was composed by: (1) the panel skin, (2) the stringers, (3) the dummy frames and (4) the adhesive layer.

First-order reduced integration shell elements S4R were used for the skin, the stringers and the dummy frames, whereas solid elements C3D8R were employed for the adhesive layer, [6]. Regarding the size of the elements of the meshes, the use of at least 10 elements along each dent appearing at the postbuckling evolution is recommended [3]. Table 4 shows a summary of the characteristics of the meshes used.

Table 4. Summary of global mesh.

Component	No. of elements	No. of nodes	Element type	DOF	Average size
Skin	53156	53625	S4R	321750	1.83 mm
Stringer (×3)	35360	36309	S4R	217854	1.83 mm
Frames (×4)	4900	5111	S4R	30666	1.83 mm
Adhesive (×6)	14682	32806	C3D8R	98418	1.83 mm

In order to reproduce the supporting conditions of the experimental test, several features were included:

- A multipoint constraint was used at the lower axial extreme of the panel. This constraint restricted all the nodes around the bottom region of the panel to move acording to the displacements of a master point placed at the geometrical centre of that section, which was only allowed to translate along the axial direction.
- Analogously, another multipoint constraint was used at the upper axial extreme of the panel. In this case, the corresponding master point had all its degree of freedom restrained.
- The lateral guides were modeled restraining the traslation perpendicular to the skin at all the nodes of the lateral sides of the skin frame.
- The actions of the rods supporting the flange of the frames were modeled restricting the radial traslation of all the nodes belonging to corresponding flanges.

Excerpt from ISBN 978-3-00-053387-7

- Abaqus® *TIE constraint were used to connect the meshes of the parts of the panel (skin, stringer, adhesive and frames), which were non conforming each other. This constraint type simulates perfect inferface.

Geometrical imperfections were included in the global model by combinations of buckling modes, that were obtained in a previous analysis. In this way, the perturbed geometrical position of the node n, $x_i(n)$ ($i = 1, 2, 3$), can be expresed in the form [3]:

$$x_i(n) = x_i^o(n) + \sum_{k=1}^{m} a_k \bar{u}_i^k(n) \tag{1}$$

$x_i^o(n)$ being the ideal position of the node n, m the number of buckling modes considered in the combinations, $\bar{u}_i^k(n)$ the normalized displacement (maximum equals 1) of the node n corresponding to the buckling mode k, and a_k coeficients defining the weight of the mode k. Coefficients a_k should be computed adjusting the perturbed geometry to the actual geometry of the panel. Unfortunately, there was no information about the actual geometry of the tested panel. Thus, some combinations were considered. Here the results corresponding to the combination of buckling modes 1, 3 and 9, with $a_1 = a_3 = a_9 = 10$ mm are presented.

The problem was solved using Newton-Raphson technique, load was introduced modifying the axial displacement at the control point of the mobile extreme; initial and maximum increment was about tenth the first buckling load.

5.2. Results of the global model

Fig. 3 shows the obtained numerical (solid line) and experimental (marks) load-displacement evolution. Numerical distributions of radial displacements for two load levels are also shown in this graph. The experimental colapse load was 848 kN and the first buckling load obtained numerically was around 722 kN, thus there is a short period of postbuckling regime prior to collapse for this structure.

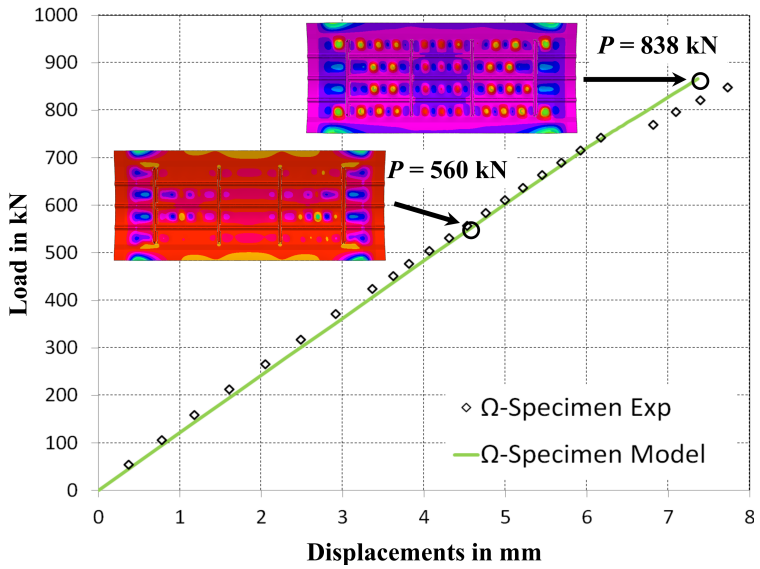

Figure 3. Global results. Correlation with experimental measures.

The computations were performed till 850 kN. Satisfactory agreement up to around a load level equal to

Excerpt from ISBN 978-3-00-053387-7

750 kN can be observed. At this load level, experimental measures seem to have a sudden drop, which is not captured by the global numerical model.

6. Local model: simulation of interlaminar damage

6.1. Local finite element model

In view of the experimental results and of the numerical distribution of internal forces obtained with the global model, three regions of the central inter-frame area of the panel, see Fig. 4, were selected for the local analyses. Each local model corresponds to one of the stringers. Dimensions ensure that several dents are included in each local model.

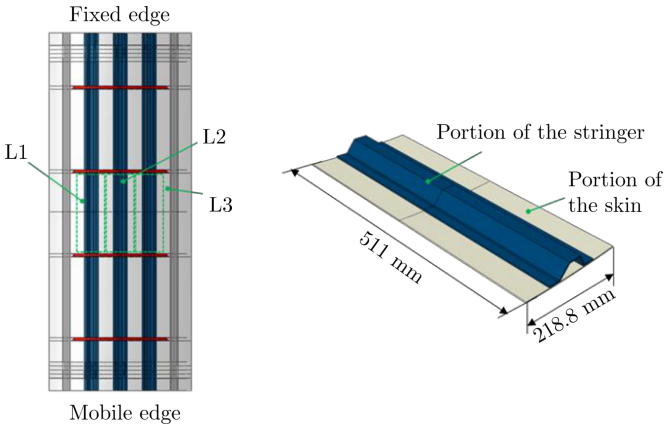

Figure 4. Local models.

Each local model was composed by the following entities: (1) skin portion, (2) stringer portion, and (3) adhesive layer. Table 5 summarizes the characteristics of the mesh of each part. C3D8R is a first-order layered solid element with reduced integration, and COH3D8 is a first-order cohesive element. Safe regions, close to the extremes (≤ 5 mm) of the adhesive layer, were considered to prevent potential local effects on the damage estimation due to boundary conditions. Notice that stringer and skin meshes are non-conforming with adhesive mesh. Abaqus® `*TIE` constraints were used to join skin and stringer with the adhesive layer.

Table 5. Summary of the local mesh.

Component	No. of elements	No. of nodes	Element type	DOF	Average size
Skin	113664	143920	C3D8R	431760	1.0 mm
Stringer	120064	139808	C3D8R	419424	1.0 mm
Adhesive (cohesive)	94200	208692	COH3D8	626076	0.2 mm
Adhesive (elastic)	8000		C3D8R		0.2 mm

Cohesive element behavior follows a bilinear law, with the properties shown in Table 3. 3D version of the Benzeggah-Kenane failure criterion is considered for mixed mode fracture toughness [10].

Local models (L1, L2 and L3 in Fig. 4) were solved using initial and maximum load step equals 1 kN.

Excerpt from ISBN 978-3-00-053387-7

They reached the final load, 850 kN, without excesive convergence difficulties in achieving equilibrum.

6.2. Results of the local models

Fig. 5 shows the damage parameter (scale varies from 0 = undamaged to 1 = debonded, and colors from blue to red) distribution around the adhesive layers for four load step: (1) 700 kN, before the jump in experimental measures; (2) 750 kN in the vicinity of the jump; (3) 800 kN, after the jump; and (4) 850 kN, the final load.

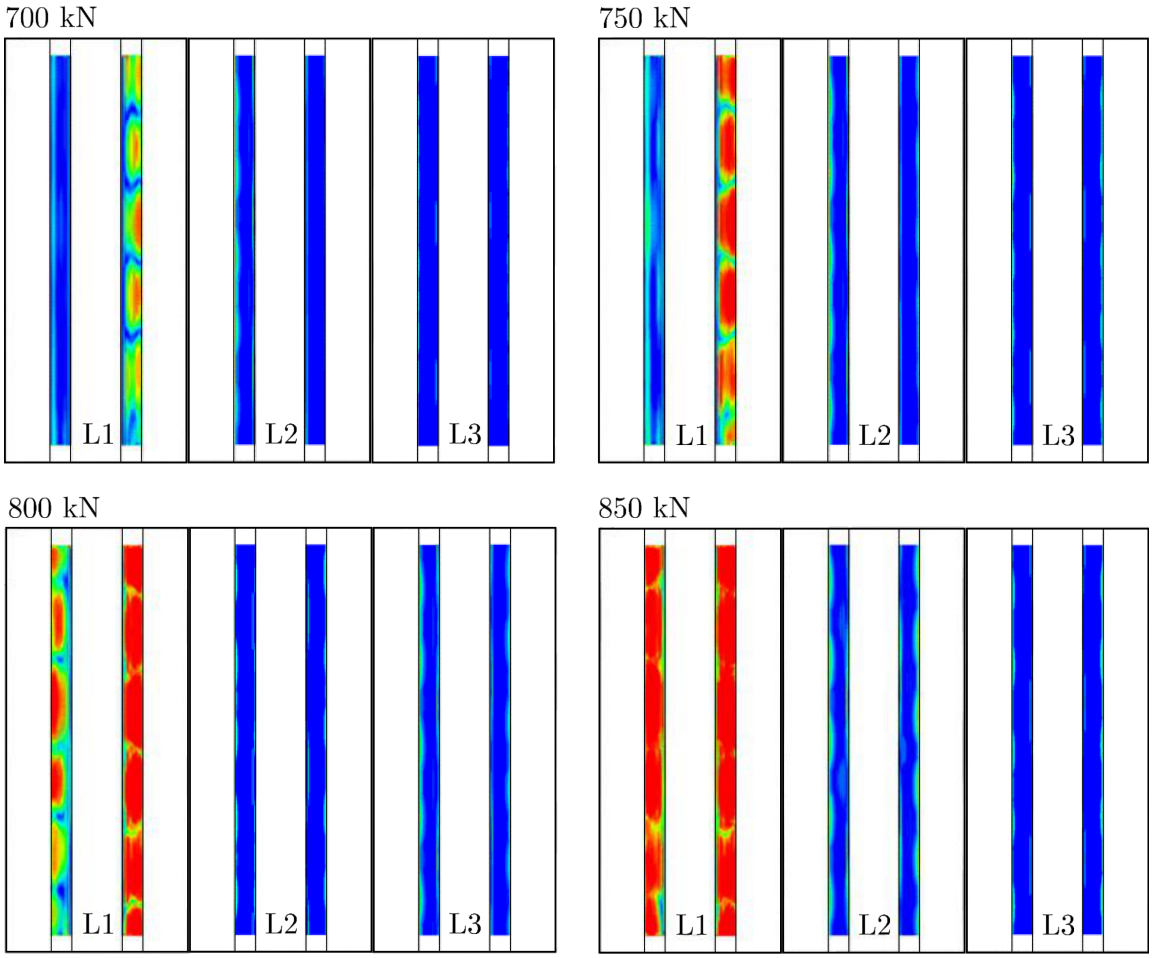

Figure 5. Damage estimation around de adhesive layers for several load levels.

At 700 kN the interface under the internal foot of the stringer L1 was partially damaged (damage parameter greater than 0 and lesser than 1) although debonding was not evident yet (damage parameter equals 1). It is worth to be mentioned that for this load level, debonding was not detected in the test by ultrasonic inspection. At 750 kN damage progressed quickly under this foot and extensive debonding appeared, this load corresponds with the jump detected along the load vs. displacement experimental evolution, see Fig. 3. For 800 kN, damage appeared under the external foot of stringer L1 and extended quickly, additionally, onset damage (no debonding yet) appeared under feet of stringers L2 and L3. For 850 kN most of the interface between both feet of stringers L1 and the skin was completely debonded, while damage around the feet of stringers L2 and L3 grew slowly. All these predictions were in accordance with the experimental evidences.

Excerpt from ISBN 978-3-00-053387-7

7. Conclusions

A multi-stringer panel has been analyzed from numerical and experimental points of view. Submodeling global-local strategy was used to simulate numerically the behavior of the panel. Both levels of analysis consider geometrical non-linearities, perturbation of the geometry was only considered at the global level, while interface damage was only modeled at the local one. Actual geometry of the panel was not measured, thus several combinations of buckling modes having been considered for the analysis.

Agreement between numerical predictions and experimental measures is satisfactory during the prebuckling and the initial stages of the postbuckling regime. At advanced postbuckling stages, correlations quality decreases. These discrepancies have, at least, two reasons: (1) the lack of knowledge about the actual geometry of the particular tested panel (which affects seriously the predictions), and (2) the absence of feedback from the local model to the global one in order to consider the efect of the damage in the global evolution. Nevertheless, onset and characteristic of damage were correctly predicted.

Acknowledgments

This work was supported by the Spanish Ministerio de Economía y Competitividad (projects DPI2012-37187 and MAT2015-71036-P) and the Andalusian Government (Project TEP-7093). The authors are grateful to AIRBUS/Spain and to the staff of TEAMS for the information on the experimental program.

References

[1] C Bisagni, P Cordisco. Post-buckling and collapse experiments of stiffened composite cylindrical shells subjected to axial loading and torque. *Composite Structures* 73:138-49, 2006.

[2] H Abramovich, T Weller, C Bisagni. Buckling behavior of composite laminated stiffened panels under combined shear-axial compression. *Journal of Aircraft* 45:402-13, 2008.

[3] A Blázquez, J Reinoso, F París, J Cañas. Analysis in the postbuckling regime of a pressurized stiffened panel Part II: Numerical analysis and effect of the geometric imperfections. *Composite Structures* 94:154454, 2012.

[4] KA Stevens, R Ricci, GO Davies. Buckling and postbuckling of composite structures. *Composites Part B: Engineering* 26:18999, 1995.

[5] BG Falzon, KA Stevens, GO Davies. Postbuckling behaviour of a blade-stiffened composite panel loaded in uniaxial compression. *Composites Part A: Applied Science and Manufacturing* 31:45968, 2000.

[6] ABAQUS V6.12 (2012) Analysis users manual, Dassault Systèmes Simulia Corp.

[7] J Reinoso, A Blázquez, F París. Damage simulations in composite structures in presence of stress gradients. *In: Modelling Damage, Fatigue and Failure of Composite Materials*, R. Talreja and J. Varna edts, 2016.

[8] AC Orifici, RS Thomson, I Herszberg, T Weller, R Degenhardt, J Bayandor. An analysis methodology for failure in postbuckling skin-stiffener interfaces. *Composite Structures* 86:18693, 2008.

[9] R Krueger, JG Ratcliffe, PJ Minguet. Panel stiffener debonding analysis using a shell/3D modeling technique. *Composite Science and Technology* 69:235262, 2009.

[10] PP Camanho, C Dávila, MF de Moura. Numerical simulation of mixed-mode progressive delamination in composite materials. *Journal of Composite Materials* 37:1415-38, 2012.

Excerpt from ISBN 978-3-00-053387-7